Jurnal Kejuruteraan 36(6) 2024: 2273–2286
https://doi.org/10.17576/jkukm-2024-36(6)-03

Exploring The Behaviour of Dapped Wet Wall-To-Wall Connections Under Uniformly Distributed Load

(Meneliti Perilaku Sambungan Basah Dinding-ke-Dinding yang Dikenakan BebanTeragih Seragam)

Amril Hadri Jamaludin[a], Noorsuhada Md Nor[a*], Muhhamad Nur Aizuddin Amrin[a], Amir Khomeiny Ruslan[a], Ahmad Syauqi Md Hassan[a], Soffian Noor Mat Saliah[a], Muhammad Afiq Tambichik[b], Mohd Azrizal Fauzi[a] & Shahrum Abdullah[c]

[a]*Civil Engineering Studies, College of Engineering, Universiti Teknologi MARA Cawangan Pulau Pinang, Permatang Pauh Campus, Pulau Pinang, Malaysia.*

[b]*Pusat Kecemerlangan Kejuruteraan dan Teknologi JKR (CREaTE), Alor Gajah, Melaka, Malaysia*

[c]*Department of Mechanical and Manufacturing Engineering, Faculty of Engineering and Built Environment, Universiti Kebangsaan Malaysia, UKM Bangi, Selangor, Malaysia*

[*]*Corresponding author: ida_nsn@uitm.edu.my*

Received 8 March 2024, Received in revised form 5 July 2024
Accepted 14 August 2024, Available online 30 November 2024

ABSTRACT

The connection between two wall panels is the weakest part of the wall system and becomes the crucial point of failure. This paper presents the behaviour of two proposed types of wall-to-wall connections subjected to uniformly distributed load until failure, dapped wet and lightly vertically reinforced dapped wet connections. A total of twelve wall panels were prepared and constructed as six wall-to-wall connections, with three connections for each type. The acoustic emission (AE), maximum load (P_{max}), strain and deflection characteristics were analysed and discussed to determine the behaviour of each wall-to-wall connection. The occurrence of cracks on the walls during the tests was also observed. The results showed that the P_{max} for the wet and lightly vertically reinforced wall-to-wall connections of dapped concrete were 164.37 kN and 138.44 kN, respectively. From the distribution of AE, the highest energy was determined for the lightly vertically reinforced wall-to-wall connection, at 18000 eu. From the AE activity mapped on the crack pattern, it was observed that most AE activities occurred at the top of the wall, which corresponded strongly with the occurrence of cracks at the wall connection surface. Vertical cracks occurred in the connection areas, propagating from the top to the bottom. The major benefit of this study is the proposal for a new type of vertical wall-to-wall connection that can be used in prefabricated wall panel systems in industrialised building systems.

Keywords: Dapped connections; Industrialised Building System; precast wall panel; recycled concrete aggregate; uniformly distributed load; Acoustic Emission technique

INTRODUCTION

The construction industry has adopted the Industrialised Building System (IBS) to improve construction quality and productivity (Mohd Amin et al. 2017), with many countries now attempting to employ the IBS. Modern Methods of Construction (MMC) in the UK are described as technologies that provide an efficient approach to preparing more production in less time (Vaghei et al. 2014). In construction, these include prefabricated technologies, off-site manufacture and offset fabrication. In Malaysia, the IBS refers to the process of manufacturing an element in a controlled environment, transporting it and assembling it at the main site (CIDB Malaysia, 2017). Walls are the most common application for precast concrete elements in

the construction of buildings. Precast concrete walls are ideal for low- to medium-rise commercial and industrial buildings. They are generally easy to manufacture, efficient, durable and desirable (Vaghei et al. 2014). Moreover, precast concrete is the most used IBS system in Malaysia. The most important factor to consider in the IBS is the connection between two wall panels.

This connection is a serious matter and worthy of consideration as many failures occur at this location. Inamdar (2018) stated that the connection between structural elements is the weakest part of the structure due to the interaction between two or more elements. Difficulties have been encountered in aligning and transporting the heavy precast elements used in the IBS during assembly at construction sites. This leads to future problems such as leaks and cracks due to improper post-construction assembly, affecting the quality and function of the building and its end users. Although these are the most critical process aspects, the design and construction of precast concrete structures and buildings can be problematic (Inamdar, 2018). As wall panels are joined at the connections, the overall building performance depends on the efficiency of these connections. Wall-to-wall connections are hugely important as they provide the structural integrity and strength of the entire building system. Therefore, the connections must be able to maintain their stability and structural integrity during serviceability and the ultimate limit state, as well as provide continuity between connected sections (Abdullah et al. 2019). Therefore, these connections should be thoroughly investigated to ensure the efficiency of the IBS.

Various forms of wall-to-wall connections, as well as dry and wet connections, are used in buildings. The latter are made of cast-in-place concrete or composite materials poured or injected between precast concrete wall panels (Brzev & Guevara-perez 2021). The type of wall panels used determines the choice of connection (Artemeva, 2018). Currently, loop connections, wire rope connections and shear keys for wet joints are available for wet connections, among others. Steel fibres have been used in wet joint shear keys, but they increase the crack development and peak shear loads along the joint interface between connected panels (Ahilan et al. 2016). Loop connections are far more suitable than bolted connections as they are easily installed on site and do not require professional services, unlike the latter (Abdullah et al. 2019). Despite the many types of wall-to-wall connections, some - such as the dapped wet and lightly vertical dapped wet connections - have seldom been considered. Therefore, these two types of wall-to-wall connections should be specifically studied, especially in terms of their performance.

To investigate the performance of a wall, Ruslan et al. (2021) examined its behaviour in terms of compressive strength, ultimate load, deflection and strain. Qian et al. (2021) and Pan et al. (2021) studied the cracking pattern of a wall at failure after horizontal cyclic loading; they analysed and discussed the yield load, drift ratio, loop stiffness and strain. For smaller axial load values, the load-bearing capacity was found to decrease but the deformability increased. Vaghei et al. (2014) investigated the interaction between modelled concrete and precast concrete, as well as between reinforcement and concrete, in terms of nonlinear stress-strain behaviour. The connection performance was evaluated in terms of stress, deformation and absolute plastic strain. The authors found that the crack propagation in the IBS walls and the connection occurred mainly at the bottom of the IBS wall and along the interface, while the in-plane lateral loads resulted in some cracks at the connection between the IBS walls and the connection. The review clearly revealed that the performance of wall-to-wall connections had only been investigated to a limited extent; however, limited use had been made of non-destructive testing for this purpose, such as the acoustic emission (AE) technique.

The AE technique is often used to identify the integrity of reinforced concrete beams (Md Nor et al. 2022; Mat Saliah & Md Nor 2022; Mat Saliah et al. 2021; Noorsuhada 2016), detect the compactness of socket grouting in shear walls (Li et al. 2021), detect fatigue cracks in the eyebars of steel bridges (Megid et al. 2019) and monitor concrete slab-to-wall connections (Reboul et al. 2020). Ospitia et al. (2023) found AE to be a highly promising form of real-time assessment of material condition before the load-bearing capacity was compromised. The review revealed the limited use of the AE technique to study the behaviour and performance of concrete wall-to-wall connections. Therefore, the main objective of this study was to investigate the behaviour and performance of dapped concrete wall-to-wall connections under uniformly distributed load. Two types of dapped wet vertical wall-to-wall connections were proposed. The behaviour of each wall-to-wall connection was evaluated by analysing the compressive strength, deflection, stress, strain and cracks that developed on the wall. The AE characteristics were used to assess the cracking behaviour of the wall-to-wall connections.

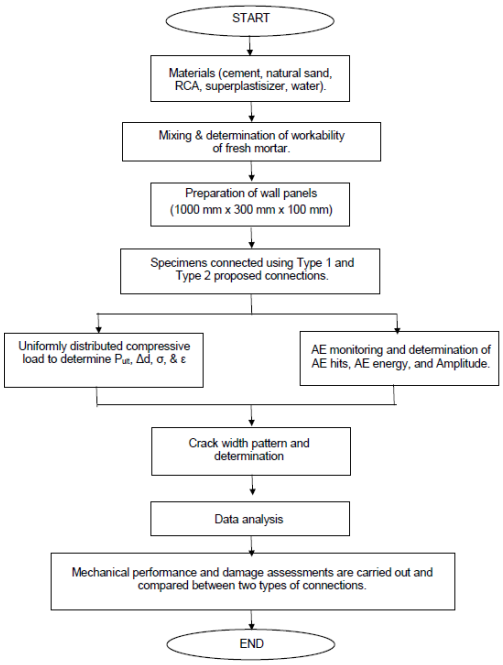

FIGURE 1. Process flow for the determination of the mechanical performance and damage assessments between two proposed wall-to-wall connections

METHODOLOGY

The process flow of evaluating the behaviour of two types of wall-to-wall connections is shown in Figure 1. It started with the preparation of materials such as recycled concrete aggregate, cement, natural sand, superplasticiser and water. All the materials were mixed and the workability of the fresh mortar was determined. Wall panels were prepared with the dimensions of 1000 mm high x 300 mm wide x 100 mm thick. Two panels were joined using the two proposed connections: Type 1 (Dapped wet) and Type 2 (Lightly reinforced dapped wet). Each hardened wall-to-wall connection was tested and cracks were monitored using the acoustic emission technique. The ultimate load, deflection, stress, strain and acoustic emission energy were then obtained. Thus, the mechanical performance of the two types of connections could be determined.

MATERIAL AND SPECIMEN PREPARATION

In this study, recycled concrete aggregate (RCA) was used to replace 50% of the natural fine aggregate in the mortar mix. The RCA was extracted from tested concrete cubes at a batching plant in Penang. These cubes were crushed with a jaw crusher into fine aggregates that fit through a 5 mm sieve. The other raw materials used for the mortar mix were ordinary Portland cement (OPC), water free of impurities and natural fine aggregates that fit through a 5 mm sieve. In total, 12 mortar cubes measuring 50 mm x 50 mm x 50 mm were cast in a 1:2:2 ratio of cement: RCA: natural fine aggregate. To improve the mortar's workability, 11.49 ml of superplasticizer, namely Sika ViscoCrete 2192 was added to the mortar mix, based on the manufacturer's recommendation. All the cubes were used to determine the compressive strength of the mortar at 3, 7, 14 and 28 days. The compressive strength test indicated that the average compressive strength of the mortar at 28 days was 17.87 MPa.

A total of 12 formworks measuring 1000 mm high x 300 mm wide x 100 mm thick were made to prepare the wall panels. The formworks were used to pour the wall panels, with the proposed connection shape and dimension formed using the Styrofoam method at one end of the form. The fresh mortar was mixed in a concrete mixer, poured into the prepared formwork in three layers and compacted with a vibrator to ensure that the entire mixture was evenly distributed in the formwork and well compacted to avoid subsequent honeycombing. All the poured test specimens were cured in a laboratory, with moistened bags placed on the specimens.

After all the wall panels had been cured for 14 days, the wall panels were connected in the form of vertical wall-to-wall connections, with a concrete grout used as the bonding agent between pairs of panels. Two types of connections were prepared, namely, Type 1 for dapped wet and Type 2 for lightly reinforced dapped wet. Three test specimens each of Type 1 (Dapped wet) and Type 2

(Lightly reinforced dapped wet) were formed, as presented in Table 1. Thus, three specimens were produced for each type. T1 and T2 were designated as the types of wall-to-wall connection, while S1, S2 and S3 were designated as the specimen numbers. Thus, the Type 1 connections were named T1S1, T1S2 and T2S3, while the Type 2 wall-to-wall connections were named T2S1, T2S2 and T2S3.

The cement grout used was SikaGrout-215, which has a compressive strength of more than 45 MPa after seven days of casting with mortar in castable form, according to ASTM C109M-02 (2020). The bonded wall panels continued to be cured for the remaining 14 days. On the 28th day, testing was conducted to determine the mechanical performance of the wall-to-wall connections. The damage to each specimen was also assessed using the acoustic emission technique.

Figure 2 shows the schematic diagram of the proposed vertical wall-to-wall connections. In the case of the slightly reinforced wet wall, two vertical steel bars were inserted at a specific spacing, as shown in Figure 2. The steel bars were used to reinforce the connection part of the joint. Figure 3 shows the prepared wall panels before the joining process.

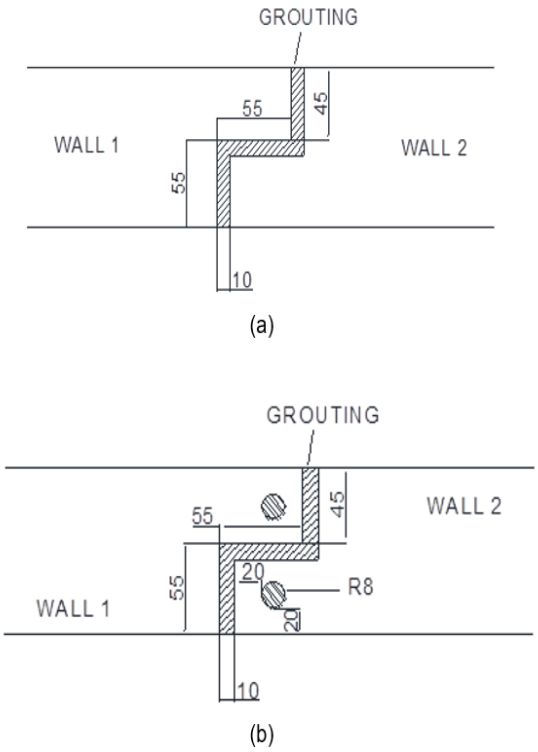

FIGURE 2. Schematic diagram of proposed vertical wall-to-wall connection in plan view. (a) Type 1 (Dapped wet), and (b) Type 2 (Lightly reinforced dapped wet)

FIGURE 3. Curing of the wall panels

TABLE 1. Types of wall-to-wall connections

Types of connection	Specimens	Size (mm) / pair
Type 1: Dapped Wet	T1S1	1000 mm x 535 mm x 100 mm
	T1S2	
	T1S3	
Type 2: Lightly vertical reinforced dapped wet	T2S1	
	T2S2	
	T2S3	

TEST SETUP

Figure 4 shows the schematic diagram of the test setup of the wall-to-wall connections and illustrates the arrangements made for other measurements, such as linear vertical displacement transducers (LVDTs), strain gauges and AE sensors. The LVDTs were used to measure deflection at selected locations and strategically positioned on the wall panel surfaces, 240 mm (designated as D1) and 490 mm (designated as D2) from the top of each specimen, respectively, as shown in Figure 5. This was to record the horizontal displacement when uniformly distributed load was applied to the top surface. The strain gauges were located at 250 mm (fourth quarter of the wall height) and 500 mm (half the wall height). They were designated as SG1 and SG2, as shown in Figure 5. SG1 was placed at 250 mm to record the strain at the connection interface and SG2 was placed at 500 mm to record the strain in the dapped area. Four AE sensors were fixed at selected locations and designated as CH1, CH2, CH3 and CH4, as shown in Figure 5. Each specimen was held in a fixed position on the test platform and uniformly distributed load was applied on top of the wall-to-wall connection. The wall-to-wall connections were statically loaded to failure at a constant load rate of 0.1 mm/min. The crack pattern

of each wall-to-wall connection was also investigated. The same test method used in Jamaluddin et al. (2023) was also used for this study.

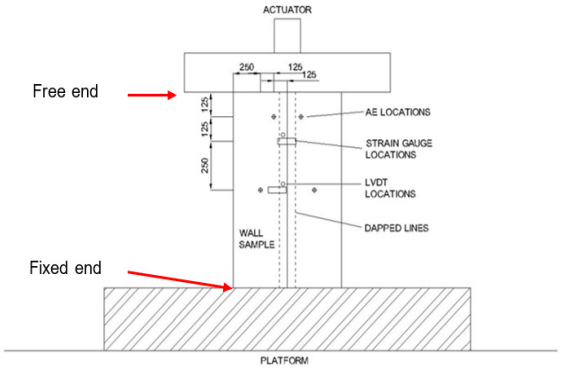

FIGURE 4. Schematic diagram of the wall-to-wall connection setup with other instruments (units in mm)

ACOUSTIC EMISSION MONITORING

Acoustic emission (AE) was used to monitor the crack propagation in each specimen when uniformly loaded to failure. As acoustic emission is defined as elastic wave propagation due to localised internal energy release, this allows the identification of microfractures in elastic materials that cannot be determined visually, such as hairline cracks (Md Nor, 2018). Hence, the crack propagation in the concrete was captured and displayed on the AE display. Meanwhile, AE would be able to capture the formation of any micro and macro cracks occurring both in the mortar matrix and on its surface.

Four VS75-V sensors were placed on one side of each specimen (see Figure 4). The coordinates of the sensors are shown in Table 2, with the x and y positions indicated, while the x and y positions can be seen in Figure 5. Both CH1 and CH2 were used to detect crack initiation and propagation at each connection. Sensors CH3 and CH4 were used to detect cracking in the dapped section of the wall panels.

Before the monitoring process, the AE hardware was set in the system, as were the threshold level, wave velocity, rearm time, sampling rate, duration and discrimination time, pre-trigger and digital setting. The settings used were 45 dB, 4000 m/s, 1.62 ms, 10 MHz, 400 µs, 200 and 25 kHz to 850 kHz, respectively.

TABLE 2. Location of the sensors with the x and y coordinates on the specimen

Designation of sensor	Coordinates	
	x (mm)	y (mm)
Sensor 1, CH1	185	125
Sensor 2, CH2	360	125
Sensor 3, CH3	125	495
Sensor 4, CH4	420	495

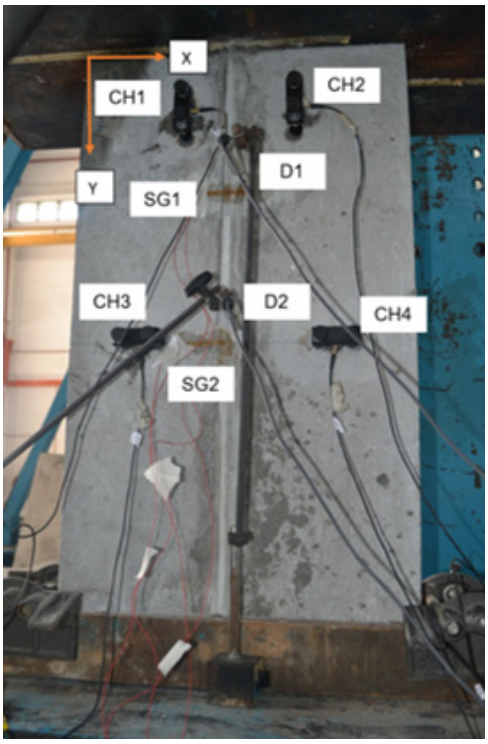

FIGURE 5. Test setup of vertical wall-to-wall connection

ANALYSIS METHOD

To determine the behaviour of the wall-to-wall connections, the stress, strain and deflection were analysed. The relationship between the load and deflection at 240 mm from the top of the wall was recorded, analysed and discussed. The stress-strain relationship was also analysed to investigate the behaviour of the connection under static loading until failure.

The crack pattern of each wall-to-wall connection was observed visually using torchlight. The crack that opened when load was applied to the top of a specimen was

observed using a crack width microscope to ascertain the exact width of the crack. The crack pattern that appeared on the sample surface was then mapped using AE features such as energy, amplitude and hit. The relationship between the x and y locations of the AE hits was also investigated. Thus, the crack locations could be verified in conjunction with the AE characteristics.

RESULT AND ANALYSIS

STRENGTH OF WALL-TO-WALL CONNECTION

Table 3 shows the performance of two types of wall-to-wall connections subjected to uniformly distributed load on the top of each specimen. This performance is presented based on the maximum load (P_{max}), deflection and moment. In this study, two LVDTs were set at 240 mm and 490 mm to measure the deflection of each wall-to-wall connection. Meanwhile, two strain gauges were fixed to each connection at 250 mm and 500 mm from the top of the wall. The strain gauges were used to measure the strain at these two locations.

From Table 3, Figure 6(a) and Figure 6(b), the horizontal deflection at a distance of 240 mm generally had a larger horizontal deflection than at 490 mm from the top of the wall. Therefore, the deflection at 240 mm is discussed in detail in this paper. Figures 6(a) and 6(b) show the relationships between load and deflection for the Type 1 and Type 2 specimens, respectively. As Figure 6(a) and Table 3 illustrate, for Type 1 (the dapped wet wall-to-wall connection), the maximum loads, P_{max} of this connection were 126.06 kN, 100.33 kN and 219.63 kN for specimens T1S1, T1S2 and T1S3, respectively. The highest P_{max} for this wall-to-wall connection was applied to T1S3, compared to the other specimens, and the average P_{max} was 148.68 kN.

As shown in Figure 6(b), for Type 2, the P_{max} values were 203.71 kN, 173.11 kN and 176.03 kN for specimens T2S1, T2S2 and T2S3, respectively. T2S1 experienced the highest P_{max} compared to the other specimens and the average P_{max} for this type of wall-to-wall connection was 184.28 kN. Following the investigation of these two types of wall-to-wall connections, the average P_{max} for Type 2 was found to be higher than for Type 1. This was due to the vertical steel bar located 20 mm from the dapped connection interface (Figure 2 (b)) to strengthen the connection. Hence, the inclusion of the vertical R8 reinforcement bar along the height of the specimen increased its strength. However, in terms of the relationship between load and deflection, the findings indicated that as load increased, the deflection also increased. Similar findings were obtained by Ruslan et al. (2021), who found that the deflection of wall panels was closely related to the load acting on the wall.

Table 4 presents the strain at 250 mm and 500 mm from the top of the specimen, as well as the axial strain and modulus of elasticity, of the wall-to-wall connections. Figures 7(a) and 7(b) show the relationship between stress and strain for the Type 1 and Type 2 wall-to-wall connection specimens. In general, higher strain occurred at the 250 mm location compared to the 500 mm location. This behaviour was consistent with the effective length of the wall principle, whereby if the free end of a structure is fixed, as shown in Figure 4, the maximum deflection occurs on the side of the free end, which in this case was at the top of the specimen. This increased the strain value near the top of the specimen recorded by strain gauge SG1, which was 250 mm from the top, compared to the value recorded by strain gauge SG2, which was 500 mm from the top. This was because the greater the deflection, the greater the likelihood that cracks would occur in the brittle material of the mortar, which in turn resulted in higher strain values being obtained from the strain gauges.

TABLE 3. The performance of the wall-to-wall connection subjected to uniformly distributed load

Type of Connections	Specimens	P_{max} (kN)	Maximum deflection at point 240 mm (mm) from the top	Maximum deflection at point 490 mm (mm) from the top	Axial deflection (mm)	Moment at (kNm)
Type 1: Dapped Wet	T1S1	126.06	8.42	3.59	4.5	1.06
	T1S2	100.33	5.45	2.26	2.8	0.55
	T1S3	219.63	4.88	2.78	6.6	1.07
	Average	148.68	6.24	2.88	4.63	
Type 2: Lightly vertical reinforced dapped wet	T2S1	203.71	5.54	2.39	5	1.13
	T2S2	173.11	8.96	4.87	-	1.55
	T2S3	176.03	3.98	1.10	3.4	0.70
	Average	184.28	6.16	2.78	4.2	

TABLE 4. The strain and performance of the wall-to-wall connection subjected to uniformly distributed load

Type of Connections	Specimens	Maximum strain at 250 mm from the top (SG1) (μmm/mm)	Maximum strain at 500 mm from the top (SG2) (μmm/mm)	Axial strain (μmm/mm)	Modulus of elasticity (kPa)
Type 1: Dapped Wet	T1S1	274	433	2.248	0.0287
	T1S2	1781	186	1.415	0.0275
	T1S3	197	86	3.291	0.0277
Type 2: Lightly vertical reinforced dapped wet	T2S1	614	390	2.485	0.0266
	T2S2	-	-	-	-
	T2S3	137	64	1.715	0.0278

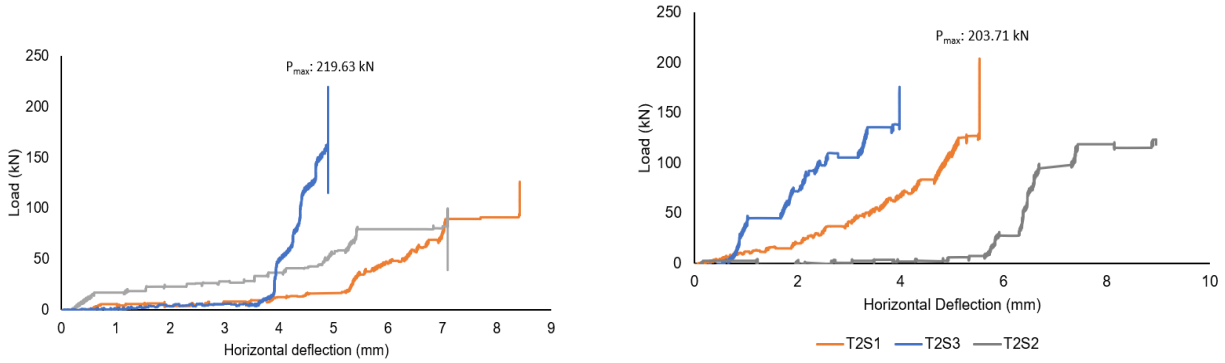

(a) (b)

FIGURE 6. Relationship between load and horizontal deflection for (a) Type 1 connection and (b) Type 2 connection, both at 240 mm from the top of the specimen

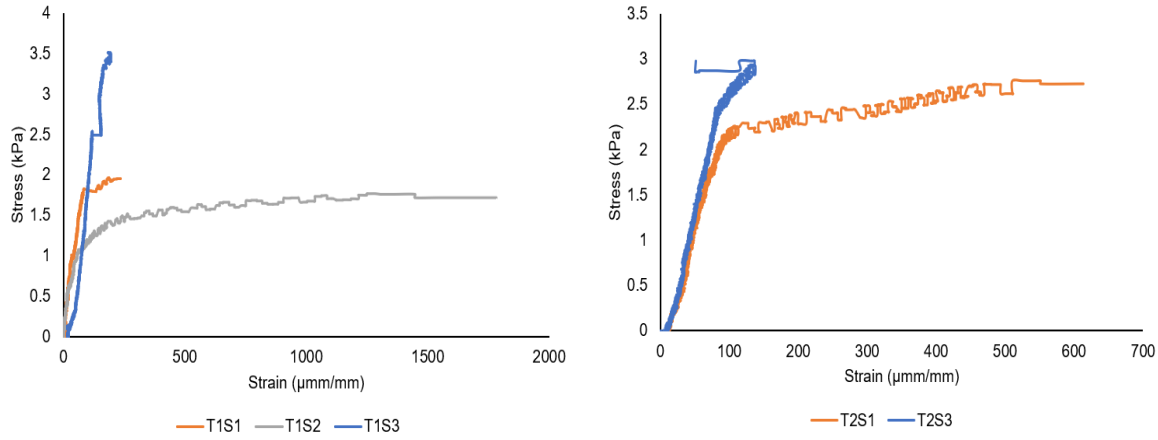

(a) (b)

FIGURE 7. Stress-strain relationship for (a) Type 1 connection and (b) Type 2 connection, both at 250 mm from the top of the specimen. Specimen T2S2 was excluded since there was a malfunction on the data logger during the test

VISUAL INSPECTION OF CRACK PATTERN

Most early cracks occurred from the top of the wall at the connection in all the specimens. The cracks propagated vertically from the top to the bottom of the wall connection and occurred on both parts of the specimens. The cracks that occurred on the wall surface are coloured red. The solid yellow line represents the visible connection interface of the dapped line. The dashed yellow line represents the connection interface of the dapped line on the other side of the specimen. To ensure the crack patterns were traced correctly, a grid of 20 mm x 20 mm was drawn on each specimen. Figures 10 and 11 show the crack pattern of the connection for the wall-to-wall connections of Type 1 and Type 2, respectively.

The crack patterns of all the specimens indicated clearly that the crack width in the upper part of the wall connection was larger than in the lower part. This was related to the first crack that appeared at the top of the wall and slowly propagated to the lower part of the wall. Figure 8(a) clearly shows that for the Type 1 (the dapped connection using specimen T1S1), a single crack appeared on the wall surface The crack had a width of 0.65 mm and occurred at 150 mm from the top of the wall. The crack width decreased to 0.45 mm at a distance of 250 mm from the top of the wall. At 410 mm from the top, the crack width was 0.35 mm. This showed that a larger crack occurred in the upper part of the wall than in the lower part.

A similar crack pattern to that of specimen T1S1 is shown in Figure 8(b) for the wall-to-wall connection specimen T1S2, in which a single crack with a width of 1.4 mm appeared 140 mm from the top of the wall. The crack width decreased to 0.85 mm at 420 mm and 0.8 mm at 700 mm, as measured from the top of the wall. This crack width was observed by enlarging it using the crack width microscope, as shown in Figure 10(a). However, the cracking in specimen T1S3 was different as many cracks occurred below the load. This started with a single crack in the connection part. As load was continuously applied on the wall, many cracks appeared in the upper part. Closer inspection of this specimen revealed excess cement grout material on the top of the specimen, where the load had been uniformly distributed. This resulted in an uneven surface coming into contact with the uniformly distributed load, so the stress increased at the location of the uneven surface, as shown in Figure 8(d). Along the top of the wall, the crack width remained constant at 1.2 mm up to a distance of 560 mm from the top of the wall. The crack width decreased to 0.4 mm at a distance of 700 mm.

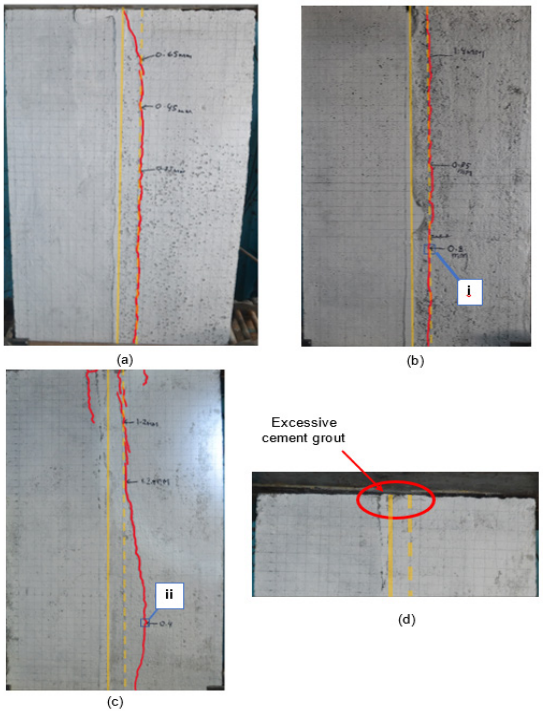

FIGURE 8. Crack pattern of the Type 1 wall-to-wall connection for specimens (a) T1S1 (b) T1S2 and (c) T1S3. (d) excessive cement grout on T1S3 created additional stress when load was applied

For Type 2 specimens, smaller crack widths were observed for two of them, namely T2S1 and T2S2. None exceeded 0.4 mm across the heights of the specimens, as shown in Figures 9(a) and 9(b). Specimen T2S3, on the other hand, exhibited excessive compression on its surface, which made visual tracking of the crack propagation difficult.

In summary, the inclusion of R8 as light reinforcement along the step line in specimen Type 2 led to an increase in the average maximum load, while smaller crack widths were observed visually than for Type 1 without reinforcement along the dapped line. The enlarged cracking for numbers (i), (ii) and (iii) is presented in Figure 10. The cracks were measured using a crack width microscope.

Figures 11 and 12 show the failures that occurred at the joints between two panels for Type 1 and Type 2. For Type 1, most failures for this type of wall-to-wall connection occurred at the dapped, not at the concrete interface or concrete grout. A similar failure pattern can be seen in Figure 12 for Type 2, the lightly vertical reinforced dapped wet. This indicated that the concrete grout was a good adhesive for the connection between two wall panels, as most of the failures with this connection occurred at the dapped.

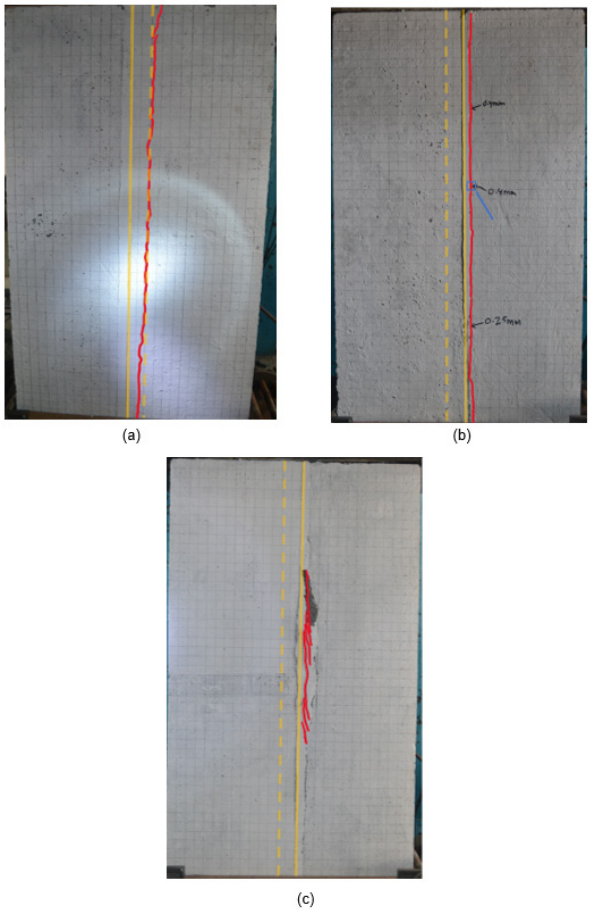

FIGURE 9. Crack pattern of the Type 2 wall-to-wall connection for specimens (a) T2S1 (b) T2S2 and (c) T2S3

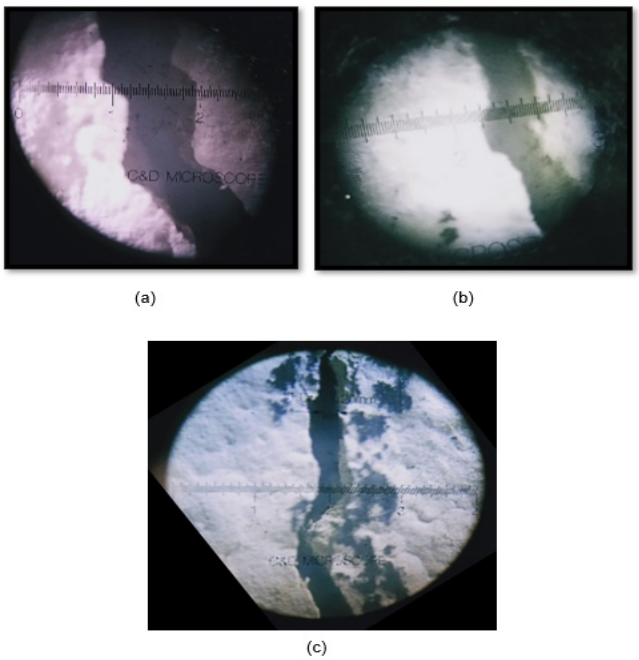

FIGURE 10. Enlargement of crack width observed using crack width microscope for samples with crack number and location number (a) T1S2 – (i) 0.8 mm, (b) T1S3 – (ii), 0.4 mm and (c) T2S2 – (iii) 0.4 mm

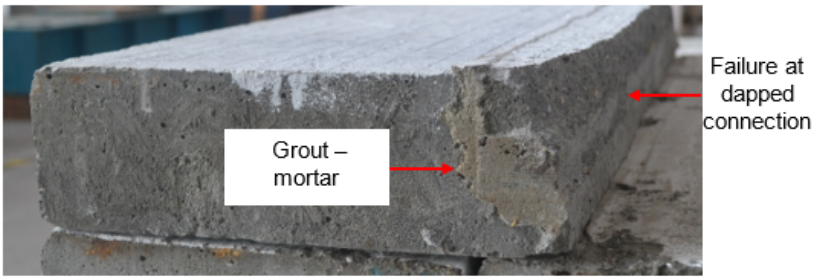

FIGURE 11. Failure of the wall connection at the joint interface of grout mortar and the dapped end for wall-to-wall connection Type 1

FIGURE 12. Failure of the wall connection at the joint interface of grout mortar and the dapped end for wall-to-wall connection Type 2

ACOUSTIC EMISSION CHARACTERISTICS

As the cracks occurred at the wall-to-wall connections from the upper to the lower parts, more acoustic emission hits along the wall can be seen in Figure 13. In this figure, the colours indicate the acoustic emission signals detected by specific sensors. Red dots indicate the signal detected by CH1, green dots are used for CH2, yellow dots are used for CH3 and blue dots are used for CH4. Most high acoustic emission hits occurred between sensors 1 and 2 since the cracks occurred at the dapped part of the connection. The locations of these high acoustic emission activities coincided strongly with the locations of the cracks that occurred on the wall surfaces, as shown earlier in Figure 9 for the Type 1. This was clearly observed when the crack pattern was transferred to the acoustic emission hits, as shown in Figure 16. High acoustic emission hits were seen on the upper part of the wall, especially along a 300 mm section from the upper part of the wall.

The high intensity of the AE hits affected CH1, with visual observation unable to show the cracks on the specimen surfaces, especially when loading began on the top of the wall, proving that the cracks or microcracks developed in the specimen matrix (Mat Saliah & Md Nor, 2022). These high AE activities coincided with the high deflection values at 240 mm, which averaged 6.24 mm for the Type 1 connection, compared to the deflection at 490 mm from the top of the wall, whose average value was 2.88 mm. Furthermore, the crack width at the nearer location with CH1 and CH2 was seen to be wider than the distance at CH3 and CH4. This showed that most cracks – both micro and macro – were formed on the top half of the specimens. Hence, the AE signal can be used to verify not only crack formation as found by but also deformation locations and crack widths (Ohno & Ohtsu 2010; Aggelis et al. 2013).

Similar acoustic emission patterns can be seen in Figures 15 and 16 for Type 2, where sensor 1, CH1, detected more signals than the other sensors. This AE signal represented the formation of cracks that were concentrated on the upper part of the wall. In general, more signals could be detected in the CH1 and CH2 area compared to that of CH3 and CH4. Meanwhile, the deflection at 240 mm was higher than at 490 mm, with average values of 6.16 mm and 2.78 mm, respectively. Regarding the crack width, the crack width in the upper part was larger than in the lower part of the wall connection.

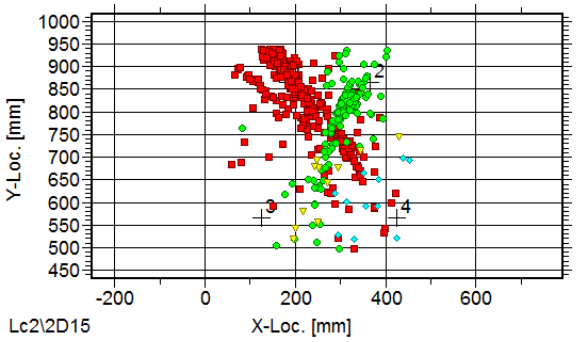

FIGURE 13. AE activities along the wall and captured by CH1, CH2, CH3 and CH4 for Type 1.

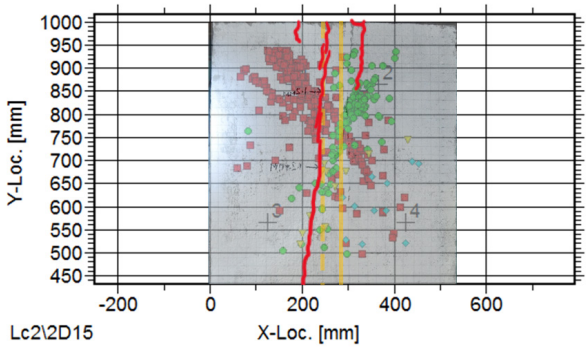

FIGURE 14. Superimposing AE hits location with flipped image for Type 1

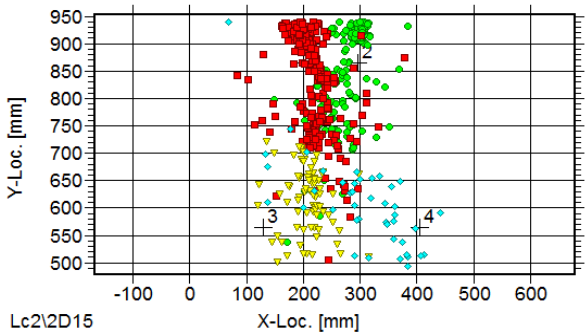

FIGURE 15. The AE activities along the wall and captured by CH1, CH2, CH3 and CH4 for Type 2

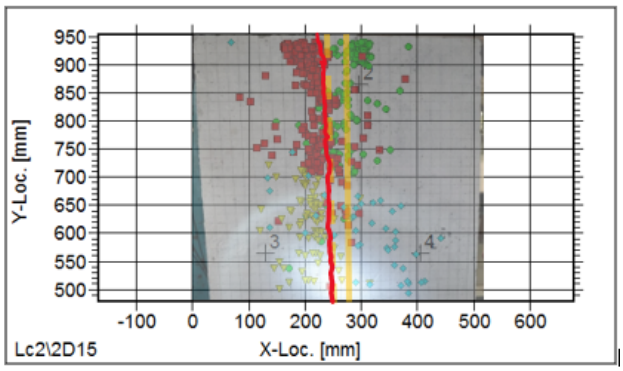

FIGURE 16. Superimposing AE hits location with flipped image for Type 2.

Figure 17(a) and 17(b) shows the crack formation that originated from the dapped section of the connection on the top of the specimen T1S3. The observed crack lines shown in Figure 14 (red line) matched the AE hits detected by CH2 (green). The highest AE energy for Type 1 (16100 eu) was found at 165 mm from the origin. Other high-intensity AE energy was detected by CH1 (red), with visual observation unable to identify the cracks on the specimen surface, proving that cracks or microcracks were formed in the specimen matrix (Md Nor, 2018). CH3 (yellow) and CH4 (blue) each registered a less intense number of acoustic emission hits than either CH1 or CH2.

This showed that most cracks, both micro and macro, were formed on the top half of the specimens. These hits were supported by the relationship between load and horizontal deflection, as shown in Figure 6(a), where D1 detected greater deflection than D2. Higher deflection values indicated greater possibilities for cracks to be formed in the specimen matrix or its surface. The same pattern was distinguished for T2S1, as shown in Figure 18(a) and 18(b), where the AE hits pattern accorded with the load, with respect to the horizontal deflection shown in Figure 6(b). The highest energy (18000 eu) was found for Type 2, as presented in Figure 18(a). The highest AE energy was due to the high stress concentration at the respective locations. Md Nor et al. (2022) stated that the high energy in the initial phase was closely associated with the formation of microcracks in concrete

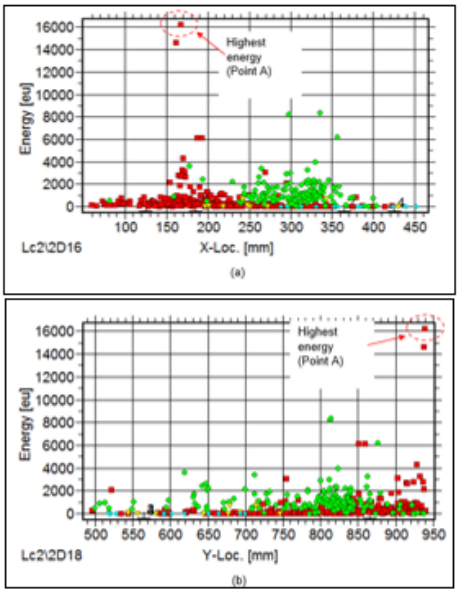

FIGURE 17. AE energy with respect to (a) X-location and (b) Y-location for Type 1

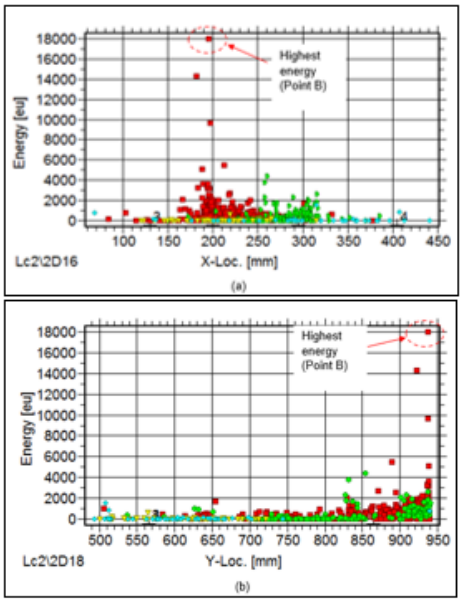

FIGURE 18. AE energy with respect to (a) X-location, and (b) Y-location for Type 2

CONCLUSION

This study has successfully proposed a new wall-to-wall connection and tested it under uniformly distributed load to further investigate the failure analysis of various connections, namely Type 1 (Dapped wet) and Type 2 (Lightly reinforced dapped wet). It was concluded that the inclusion of a simple R8 steel reinforcement arranged vertically along the specimen height produced a significant improvement in the maximum compressive capacity of the specimen when uniformly loaded to failure. The P_{max} of Type 2 (lightly reinforced dapped wet) was found to be 184.28 kN, which was higher than that of the Type 1 connection (dapped wet), whose failure load was 148.68 kN.

In addition, the crack widths in Type 2 were smaller than those of the Type 1 wall connection. This was due to the presence of the vertical steel bar in the concrete, which strengthened the wall connection when load was applied on the specimen. The observed crack patterns were successfully recorded, marked on the specimens and verified using the AE characteristics through the relationship between the energy versus the width and height of each wall-to-wall connection.

Analysis of the AE energy for the positions of both the sample width and height revealed that the highest energy occurred near the junction interface at the top of the specimens, with values of 16000 eu and 18000 eu for Type 1 and Type 2, respectively. The results corresponded strongly with the relationship between the load and

deflection of the specimens and the crack observation carried out during and after the test. Furthermore, the analysis outcomes proved that the connection interface was the weakest part of the components. The major benefit of this study is the proposal of a new type of vertical wall-to-wall connection that could be used in prefabricated wall panel systems in industrialised building systems.

ACKNOWLEDGEMENT

The authors would like to express their gratitude to Universiti Teknologi MARA, Cawangan Pulau Pinang (100-TNCPI/PRI 16/6/2 (022/2021) and Pusat Kecemerlangan Kejuruteraan dan Teknologi JKR (CREaTE) (grant no JAR 2001) for providing financial support for this research. Special thanks to Professor Dr Azmi Ibrahim, Ir Dr Sarina Ismail and all members from Jabatan Kerja Raya.

DECLARATION OF COMPETING INTEREST

None.

REFERENCES

Abdullah, M., Hasan, M., & Muhamad, R. 2019. Wall to wall horizontal connection for precast concrete structures. *International Journal of Recent Technology and Engineering* 8(3S3): 548–554. https://doi.org/10.35940/ijrte.c1097.1183s319

Aggelis, D. G., Mpalaskas, A. C., & Matikas, T. E. 2013. Investigation of different fracture modes in cement-based materials by acoustic emission. *Cement and Concrete Research* 48: 1–8. https://doi.org/10.1016/j.cemconres.2013.02.002

Ahilan, R., Nadu, T., Anandhi, S., Nadu, T., & Manager, C. E. 2016. *Experimental Investigation of Vertical Connections in Precast Wall Panel under Shear Load*. 2(12): 217–222.

Artemeva, M. 2018. Connections of wall precast concrete elements.

ASTM C109/C109M-02. 2020. Standard Test method for compressive strength of hydraulic cement mortars. *Annual Book of ASTM Standards* 04: 9.

Brzev, S., & Guevara-perez, T. 2021. Precast Concrete. *Spon's External Works and Landscape Price Book 2017*, 230–230. https://doi.org/10.1201/9781315201047-45

CIDB Malaysia. 2017. IBS Catalogue for Precast Concrete Building System Revision 2017.

Inamdar, S. M. A. 2018. Joints and connections in precast concrete buildings. *International Journal of Science and Research (IJSR)* 7(6): 881–883. https://doi.org/10.21275/ART20183152

Jamaludin, A.H., Md Nor, N., Ruslan, A.K., Mat Saliah, S.N., Abi Suhaimi, N.A.S., Md Hassan, A.S., Fauzi, M.A., & Razali, F.S. 2023. Structural performance evaluation of horizontally light reinforced dapped for vertical wall-to-wall connection of precast wall panel. *Jurnal Kejuruteraan* 35(6): 1455-1465

Li, S., Liu, X., Ma, Y., Zhang, L., & Feng, H. 2021. Influence of grouted sleeve and concrete strength of fabricated shear wall on acoustic emission detection method for sleeve compactness. *Journal of Building Engineering* 43(March). https://doi.org/10.1016/j.jobe.2021.102541

Mat Saliah, S. N., & Md Nor, N. 2022. Assessment of the integrity of reinforced concrete beams strengthened with carbon fibre reinforced polymer using the acoustic emission technique. *Frontiers in Mechanical Engineering* 8(June): 1–11. https://doi.org/10.3389/fmech.2022.885645

Mat Saliah, Soffian Noor, Md Nor, N., Abd Rahman, N., Abdullah, S., & Subri Tahir, M. 2021. Evaluation of severely damaged reinforced concrete beam repaired with epoxy injection using acoustic emission technique. *Theoretical and Applied Fracture Mechanics* 112(December 2020): 102890. https://doi.org/10.1016/j.tafmec.2020.102890

Md Nor, N., Mat Saliah, S. N., Abdullah, S., Singh, S. S. K., & Yahya, N. A. 2022. Acoustic emission characteristics for determining fatigue damage behaviour. *Structural Integrity* 25: 49–56). https://doi.org/10.1007/978-3-030-91847-7_6

Md Nor, Noorsuhada. 2018. Structural health monitoring through acoustic emission. In *Eco-efficient Repair and Rehabilitation of Concrete Infrastructures*. Elsevier Ltd. https://doi.org/10.1016/B978-0-08-102181-1.00006-X

Megid, W. A., Chainey, M. A., Lebrun, P., & Robert Hay, D. 2019. Monitoring fatigue cracks on eyebars of steel bridges using acoustic emission: A case study. *Engineering Fracture Mechanics* 211(February): 198–208. https://doi.org/10.1016/j.engfracmech.2019.02.022

Mohd Amin, M. A., Abas, N. H., Shahidan, S., Rahmat, M. H., Suhaini, N. A., Nagapan, S., & Abdul Rahim, R. 2017. A review on the current issues and barriers of Industrialised Building System (IBS) adoption in Malaysia's construction industry. *IOP Conference Series: Materials Science and Engineering* 271(1). https://doi.org/10.1088/1757-899X/271/1/012031

Noorsuhada, M. N. 2016. An overview on fatigue damage assessment of reinforced concrete structures with the aid of acoustic emission technique. *Construction*

and Building Materials 112: 424–439. https://doi.org/10.1016/j.conbuildmat.2016.02.206

Ohno, K., & Ohtsu, M. 2010. Crack classification in concrete based on acoustic emission. *Construction and Building Materials* 24(12): 2339–2346. https://doi.org/10.1016/j.conbuildmat.2010.05.004

Ospitia, N., Korda, E., Kalteremidou, K. A., Lefever, G., Tsangouri, E., & Aggelis, D. G. 2023. Recent developments in acoustic emission for better performance of structural materials. *Developments in the Built Environment* 13(November 2022): 100106. https://doi.org/10.1016/j.dibe.2022.100106

Pan, G. Bin, Cai, J., He, A., Chen, Q. J., Zuo, Z. L., He, B. Q., Tang, X. L., & Wu, H. W. 2021. An experimental study of the seismic behaviour of precast concrete shear walls with bolted-plate connections. *Engineering Structures* 248(January). https://doi.org/10.1016/j.engstruct.2021.113203

Qian, K., He, P., Deng, N., & Li, H. 2021. Impact of concrete strength on seismic behavior of T-shaped double-skin composite walls. *Engineering Structures* 236(April 2020), 112039. https://doi.org/10.1016/j.engstruct.2021.112039

Reboul, N., Grazide, C., Roy, N., & Ferrier, E. 2020. Acoustic emission monitoring of reinforced concrete wall-slab connections. *Construction and Building Materials* 259: 119661. https://doi.org/10.1016/j.conbuildmat.2020.119661

Ruslan, A. K., Nor, N. M., Kamar, M. S. H., Zainal, M. Y., Saliah, S. N. M., Ismail, S., & Ibrahim, A. 2021. The utilisation of recycled concrete aggregate as partial sand replacement in wall panel production. *Civil Engineering and Architecture* 9(6): 2018–2026. https://doi.org/10.13189/cea.2021.090630

Vaghei, R., Hejazi, F., Taheri, H., Jaafar, M. S., & Ali, A. A. A. 2014. Evaluate performance of precast concrete wall to wall connection. *APCBEE Procedia* 9(Icbee 2013): 285–290. https://doi.org/10.1016/j.apcbee.2014.01.051